Aperiodic stochastic resonance in a hysteretic population of cardiac neurons

G. C. Kember,[1] G. A. Fenton,[1] K. Collier,[1] and J. A. Armour[2]
[1]*Department of Engineering Mathematics, Dalhousie University, P. O. Box 1000, Halifax, Nova Scotia, Canada B3J 2X4*
[2]*Department of Physiology, Dalhousie University, P. O. Box 1000, Halifax, Nova Scotia, Canada B3J 2X4*
(Received 9 July 1999)

Aperiodic stochastic resonance (ASR) is studied for a densely interconnected population of excitatory and inhibitory neurons that exhibit hysteresis. Switching between states in the presence of noisy external forcing is represented as a ''competition between averages'' and this is further explained through a semianalytical model. In contrast to energy-based approaches where only the timing of a switch between states is represented, the competition between averages also identifies the input history responsible for a switch. This last point leads to some interesting conclusions regarding cause and effect in the presence of noisy forcing of a hysteretic system. For example, at subthreshold inputs, it is found that the input history causing a switch between states is primarily dependent upon the noise level even though the corresponding time to switch is sensitive to both the distance from the threshold and the noise level. Since the application considered here is to cardiac neuronal control, control performance is considered over the full input range. Noise tuning for adequate control performance is found to be unnecessary if the noise level is high enough. This is consistent with studies of ASR for sensory neurons. Another observation made here that may be of clinical significance is that at higher noise levels, constraints placed upon inputs to ensure adequate control performance are likely to depend upon the switching direction.

PACS number(s): 05.40.−a, 87.19.Hh

I. INTRODUCTION

The idea that a certain level of noise may enhance the response of a system to low-amplitude, periodic signals has been termed stochastic resonance (SR). A good introduction and literature review is available in [2]. Recently, the generalization of SR to aperiodic stochastic resonance (ASR) [3] has been applied to physiological states where the response to a low-amplitude, aperiodic, input signal is determined.

The analysis of SR and ASR has proceeded on two fronts.

(i) First, unique spectral features of the phenomenon are found. Consider systems which react only to inputs which cross a threshold. When such systems are forced by a subthreshold periodic input perturbed by noise, the noise crosses the threshold in a periodic fashion. Thus, peaks in the output power spectrum are seen near integer multiples of the forcing period. There exists an optimum level of noise which maximizes the response in the output power spectrum at the input frequency [4,5] and thus results in a maximization of the ''signal to noise'' ratio. For ASR, the cross correlation and variants [6–9] between a noisy subthreshold input and the output have been used to investigate the coherence between the input and output as a function of noise amplitude. This coherence can also be maximized at a particular level of noise (see [3] for a short review).

(ii) Second, energy models may be used to recast the system dynamics and this sometimes allows for analytical approximations to spectral features. For example, ASR has been studied in the FitzHugh-Nagumo equations [3,5]. These equations are a canonical form useful for describing the resettable firing dynamics of an excitable system such as a sensory neuron. Here, the energy description represents, by analogy, the firing of a sensory neuron as the escape of a particle from a one-dimensional potential well. In the presence of noisy forcing, Kramers's escape rate [10] may be used to describe the escape statistics, allowing the construction of an explicit approximation to the cross correlation between input and output [3]. This approach has been recently extended [11] to a noisy forcing whose intensity is modulated in terms of the input and output signals. In clinical investigations [8,12], coherence measures have been found useful to quantify the presence of ASR. Another application of ASR has been to model the increased coherence observed between a noiseless, aperiodic input and the output of chaotic maps when a control parameter is varied [13].

In this study ASR is characterized for hysteretic systems with two stable states. A well-documented example is SR applied to the magnetization response of a bistable system to a noisy, subthreshold periodic forcing exerted by an external magnetic field sweep [4]. The dynamics, in the presence of noise, is modeled using an overdamped Langevin equation where the statistics of switching between states is based upon a one-dimensional, double-welled Landau potential. ASR in a one-dimensional double-well potential is also developed in [14] by extension of the approach used to study ASR in sensory neurons [3].

Although such systems are of generic interest, attention will be focused on a physiological problem: namely, the modeling of a population of excitatory and inhibitory neurons which is densely interconnected in a redundant fashion so that the reduction may be made to a purely temporal model and input therefore to the group is ''democratic'' (the same throughout). Accumulating experimental evidence demonstrates that such populations exist in fatty tissues on the surface of the heart [16–19]. Neurons in such a population are collectively referred to as ''local circuit neurons'' [16,18]. A mathematical model is developed in [15] that shows that such a population is capable of hysteretic behav-

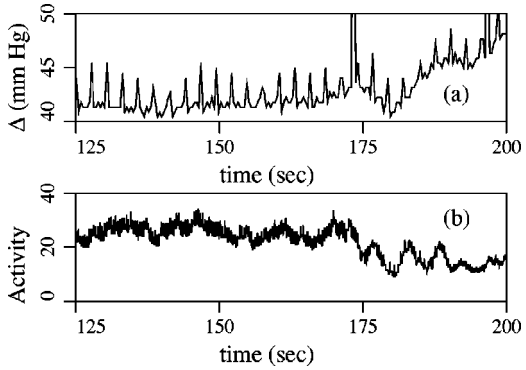

FIG. 1. Neural activity levels, constructed from raw neural measurements taken from within a local circuit are depicted with right ventricular intramyocardial pressure (RVIMP) which is measured within the heart wall tissue of the right ventricle. The neural activity levels were formed as a 2-sec moving average of the raw neural data which is sampled at 4000 Hz. The RVIMP shown here is the difference between the peak and minimum pressures during each cardiac cycle (the peaks occurring about every 2 sec are due to forced respiratory ventilation and three of these peaks are clipped). A chemical stimulant was applied to the epicardium (surface of the heart) at a time of 170 sec. An enduring shift in neural activity is observed about 3–5 sec after this stimulation, closely followed by a change in RVIMP.

ior. Qualitative experimental evidence of hysteretic behavior found in local circuit neurons is depicted in Fig. 1 where enduring shifts in neural activity are seen to occur some time after a population is subjected to a sufficient, approximately constant input stimulus.

These local circuit neurons are important to cardiac control, since they interpret inputs from cardiac afferent neurons and higher centers which provide necessary feedback to the heart [16,18]. The importance of hysteresis is that multiple steady states in activity may be used by the local circuit neurons as a means to map inputs to appropriate outputs: in other words, the heart is an *active* participant in its own control.

The activity generated by local circuit neurons is influenced by many afferent neuronal inputs from the heart and elsewhere that, not surprisingly, display fast ''noisy'' fluctuations superimposed on slower ''deterministic'' variations [20]. In light of ASR, a question that is relevant to experimental design, data analysis, and understanding the clinical role of cardiac local circuit neurons is, what is the functional role of fast ''noise'' fluctuations?

The simplest model for local circuit neuronal function is that developed in [15] and outlined here in Sec. II (this model was previously applied to the study of local circuit neurons in [21] but in a different context). Unlike previous SR and ASR studies where only subthreshold inputs are considered, the relationship between control and hysteresis in the presence of noise (Sec. III) needs to be examined over the full range of inputs in order to evaluate cardiac control performance. Energy descriptions have been used to cast the statistics of switching in the presence of noise into a rate competition between several times (for example, these times have been related in [4] to potential well geometry). However, the neuronal population model [15] requires a difficult and somewhat cumbersome two-dimensional energy description. Hence, a different formalism for the switching statistics is derived here (Sec. IV). An interesting result arising as a consequence is that switching statistics for SR and ASR in hysteretic systems is represented as competition between a *continuous* range of time averages. The expected time to switch is used to construct constraints on noise levels that are consistent with adequate control performance in Sec. V. The clinical relevance of both ASR and hysteretic local circuit neurons to regional cardiac function is also detailed in Sec. V.

II. A NEURONAL POPULATION MODEL

The mathematical model for spatially localized populations of neurons, introduced in [15], is briefly recapitulated here. It assumes that a large population of excitatory and inhibitory neurons is densely interconnected in a redundant way. This assumption allows the elimination of the spatial component and the reduction to a purely temporal model. The proportion of cells active per unit time is chosen as the relevant neuronal variable. Averaging over refractory times leads to a coupled pair of first-order, nonlinear, differential equations:

$$t_e \frac{dE}{dt} = -E + (k_e - r_e E) S_e(c_1 E - c_2 I + R(t)),$$
$$t_i \frac{dI}{dt} = -I + (k_i - r_i I) S_i(c_3 E - c_4 I + Q(t)). \tag{1}$$

where E and I are the excitatory and inhibitory activity levels, respectively. An ''activity level'' is the proportion of cells generating action potentials per unit time t. The neuronal time constants for the excitatory and inhibitory subpopulations are t_e and t_i, both taken to be 8 msec as in [15]. The interaction between the subpopulations appears in the second term on the right-hand sides. The rate of change of E, for example, is thus affected by $(k_e - r_e E)$, which can be thought of as the total number of nonrefractory cells, and S_e, which can be thought of as the fraction of those cells that can generate action potentials. In fact, these terms have units of time multiplied by the activity level and time inverse, respectively, and so the association with ''numbers of cells'' is qualitative only. S_e is a sigmoidal response function $S_e(x) = 1/\{1+\exp[-a_e(x-\theta_e)]\} - 1/[1+\exp(a_e\theta_e)]$ and $0 \leqslant S_e \leqslant k_e \leqslant 1$. In [15] the maximum fraction $k_e = S_e(\infty)$ was introduced for the analytic simplicity that results when rescaling $S_e(\infty)$ to unity is avoided.

The net input to S_e is $c_1 E - c_2 I + R(t)$. This is the sum of local subpopulation interactions $c_1 E - c_2 I$ and an external input, or forcing, $R(t)$. An important feature of this model is the interaction that occurs between the subpopulations of neurons as a result of the feedback contained in the inputs to the subpopulation response functions S_e and S_i. For example, increased activity in the excitatory subpopulation E provides negative feedback to the same subpopulation since the inhibitory subpopulation is excited simultaneously. This interaction between excitatory and inhibitory cells provides dynamical stability consistent with that observed in the experimental setting [15].

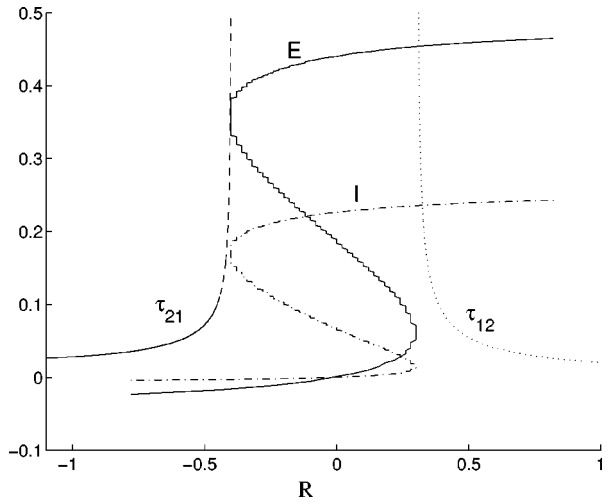

FIG. 2. The steady-state solutions E (solid line) and I (dash-dotted line), of Eq. (1) are shown as a function of a constant input forcing R. The parameters are $c_1=12$, $c_2=4$, $c_3=13$, $c_4=11$, $a_e=1.2$, $\theta_e=2.8$, $a_i=1$, $\theta_i=4$, $r_e=1$, and $r_i=1$. The time constants are $t_e=t_i=0.008$ sec. These parameters are the same as those used in Fig. 5 of [15]. The time (sec) to switch from State 1 (E and I approximately zero) to State 2 ($E\approx 0.5$ and $I\approx 0.2$) is $\tau_{12}(R)$ (dotted line) and in the reverse direction is $\tau_{21}(R)$ (dashed line).

III. HYSTERETIC CONTROL

Hysteresis is useful in closed loop control where the input is to be mapped to a finite number of output states, each of which leads to an appropriate control decision. The simplest case is that in which the output involves one of two states. This case can be considered without loss of generality since multiple states can be viewed simply as combinations of state pairs [22].

A hysteresis curve is shown in Fig. 2. In this figure, steady state solutions of Eq. (1) are depicted throughout a range of constant external forcing $R(t)=R$. The parameters of Eq. (1) are chosen such that there are only two ''states,'' characterized by approximately constant values of E and I. In addition, $Q(t)$ is taken to be zero for convenience in this solution—this restriction is discussed later. State 1 corresponds to E and I both being approximately zero. State 2 occurs when $E\approx 0.5$ and $I\approx 0.2$. If E and I are in State 1, then increasing the constant forcing R from below the threshold 0.3 to above 0.3 causes a change from State 1 to State 2 after some time. Similarly, once in State 2, a reduction of R from above -0.4 to below -0.4 results in a change from State 2 to State 1 after some time. Hysteresis in the presence of noise allows for the robust selection of states, as noted in [15], since it is somewhat resistant to state changes in the range $-0.4<R<0.3$.

This robust selection is not, however, completely adequate for control since it is also necessary to react with sufficient rapidity to changing ''essential'' control requirements. Hysteresis itself is a dynamic (or kinetic) phenomenon—the time required to change between states is sensitive to the value of the constant forcing R. The dynamic aspect is indicated in Fig. 2 where the time $\tau_{12}(R)$ required to switch from State 1 to State 2 [or $\tau_{21}(R)$ in the other direction] is shown for a constant external forcing $R(t)=R$ [23] For example, as R is increased from about $R=0.3$ to infinity, the time to switch from State 1 to State 2 is reduced monotonically from infinity to the order of the time constants t_e and t_i (taken here to be $t_e=t_i=8$ msec, as in [15]).

Another way of looking at the switching is to define a threshold $p(\tau)$, above which $R(t)$ must remain for time τ in order to result in a state switch within time τ. More specifically, if $R(t)=p(\tau)$ [$p(\tau)$ constant] from time $t=0$, then switching will occur at time $t=\tau$. Clearly $p(\tau)$ is just the inverse of $\tau(R)$. An expression for $p(\tau)$ can be found numerically from Eq. (1) by forcing them with constant $R(t)$, with $Q(t)=0$, and measuring switching times.

Aperiodic forcing model

The relationship between continuous, aperiodic, external forcing, $R(t)$ and $Q(t)$, and the output from a localized population of neurons modeled by Eq. (1) can be simplified by assuming that the forcing $Q(t)$, applied to the inhibitory neurons, is a function of the forcing $R(t)$ applied to the excitatory neurons, i.e., $Q(t)=Q(R(t))$. This produces a hysteresis curve dependent on only one variable, rather than two. Utilizing this assumption, the hysteresis curves continue to exhibit the same features as those seen in Fig. 2 when the dependence of Q on R is at least approximately monotonic and $Q(0)=0$ [15]. These requirements are not necessary, but are physically reasonable. Under these assumptions, $Q(t)=0$ will be used throughout the remainder of the paper for convenience.

The forcing function $R(t)$ is now expressed as being made up of two parts: a deterministic ''control'' function, $\overline{R}(t)$, and a mean zero random ''noise'' function $\sigma S(t)$,

$$R(t)=\overline{R}(t)+\sigma S(t). \tag{2}$$

In addition, the following piecewise constant approximation to $\overline{R}(t)$ is made:

$$\overline{R}(t)=\sum_{i=0}^{\infty} R_i[U(t-t_i)-U(t-t_{i+1})], \tag{3}$$

where $U(t)=0$, $t<0$, $U(t)=1$, $t\geq 0$, is the Heaviside step function. The assumption implicit in this approximation is that $\overline{R}(t)$ is slowly varying. More specifically, $\overline{R}(t)$ is assumed to operate at a time scale, $\min_i(t_{i+1}-t_i)$ much longer than the neuronal time constants. The usefuless of a piecewise constant approximation is that the time to switching curve $\tau(R)$ can now be used directly to determine if switching will take place in any time interval t_i to t_{i+1} under the external forcing R_i. The switching time associated with each level R_i and duration $t_{i+1}-t_i$ is specified by $\tau(R_i)$ in Fig. 2: switching will occur at some time in the interval whenever $(t_{i+1}-t_i)\geq\tau(R_i)$.

It is important to note that the switching time $\tau(R_i)$ is a property of a neuron population. It is readily identified from experimental evidence because a constant input R_i is the simplest forcing to experimentally apply and the time to switch, $\tau(R_i)$, is easily identified. Any combination of E and I can be used to infer the switching time.

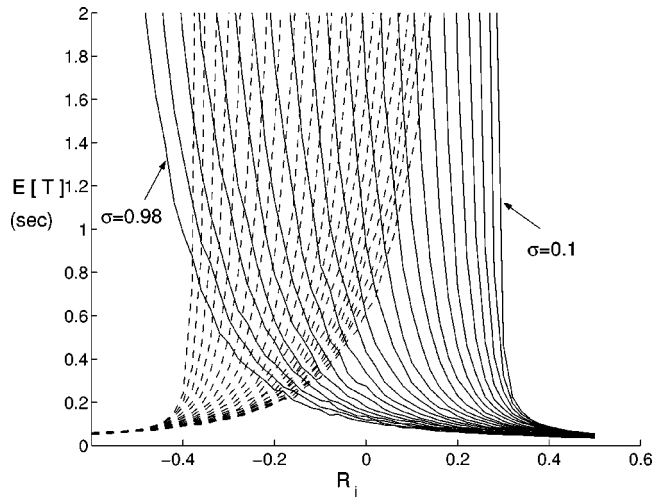

FIG. 3. The expected time to switch from State 1 to State 2 (solid lines), $E[T]$, is shown for curves of constant σ ranging from $\sigma=0.1$ to $\sigma=0.98$ with steps of $\sigma=0.04$. The same is shown for the reverse direction using dashed lines.

IV. HYSTERETIC CONTROL AND NOISE

In physical models, the external inputs to a neuronal population are typically accumulated from many sources. The most basic model for such inputs is a forcing function $R(t)$, which has a slowly varying deterministic component $\overline{R}(t)$ with superimposed noisy fluctuations $\sigma S(t)$. The latter act at, or faster, than the neuronal time constants, as discussed above. To understand the role of noise in hysteretic control, the previous discussion of switching between states in the absence of noise (Sec. III) is generalized here to switching in the presence of noisy inputs. For consistency, all results are computed using the same parameters used to produce Fig. 2.

A. Expected switching time

Fast fluctuations superimposed on the mean input R_i over the interval t_i to t_{i+1} can lead to changes in state even within the subthreshold range $-0.4<R_i<0.3$. Normally, in the absence of noise, switching will only take place in the superthreshold range $R_i>0.3$ or $R_i<-0.4$. Within the interval t_i to t_{i+1}, the noisy forcing is now taken to be $R(t)=R_i+\sigma S(t)$ where the noise component $S(t)$ is a stationary Gaussian random process with zero mean, unit variance, and exponentially decaying correlation function $\rho(\tau)=\exp\{-2|\tau|/\theta\}$. The correlation scale of fluctuation, θ, is set equal to the time constant of 8 msec to ensure that the noise is largely uncorrelated over times typically required to switch. In turn, this means that the noise itself is not, under normal circumstances, interpreted as part of the control input.

Under this stochastic model, $\tau(R_i)$ can be generalized to the expected switching time $E[T]$ which is a function of the mean input R_i and the noise variance σ^2. When $\sigma=0$, the switching time, T, becomes deterministic and equal to $\tau(R_i)$. Expected switching times for various values of σ are depicted in Fig. 3 where $\sigma=0$ is the same result as Fig. 2 for noiseless $R(t)$. Figure 3 shows the expected time to switch from State 1 to State 2 and from State 2 to State 1. The curves are obtained by simulation: 1000 realizations of $R(t)$ are input to the differential equations (1) and average switching times plotted for each mean level R_i and input variance σ^2. It is clear that the expected time to switch states is substantially reduced when $\sigma>0$ for subthreshold $-0.4<R_i<0.3$. Although not clear from Fig. 3, expected switching times appear to be slightly increased for superthreshold R_i as σ increases.

However, when σ is greater than zero, switching *reliability* also becomes *reduced* because the possibility of *cycling* between states has been introduced. The cycling period is the sum of the expected times to go from State 1 to State 2 and back from State 2 to State 1. Since the constraints of adequate control performance strike a balance between the time to switch and reliability, there will exist a range of σ producing optimum control.

Before considering more control aspects, it is useful first to develop a more specific understanding of the results in Fig. 3 using an analytical model of the expected time to switch.

B. Competition between averages

An analytical model for the expected time to switch can be developed by averaging Eq. (1). In the remainder of this section, attention will be paid only to the switch from State 1 to 2—entirely analogous mathematical developments can be made about the switch from State 2 to 1. First, $E_W(t)$, $I_W(t)$, $R_W(t)$, and $Q_W(t)$ are defined to be averages of $E(t)$, $I(t)$, $R(t)$, and $Q(t)$, respectively, over the time interval from $t-W$ to t (W is the averaging window width). For example,

$$R_W(t)=\frac{1}{W}\int_{t-W}^{t}R(\xi)d\xi. \tag{4}$$

Introduction of these averages transforms Eq. (1), to first order,

$$\begin{aligned} t_e\frac{dE_W}{dt}&=-E_W+(k_e-r_eE_W)S_e(c_1E_W-c_2I_W+R_W(t)),\\ t_i\frac{dI_W}{dt}&=-I_W+(k_i-r_iI_W)S_i(c_3E_W-c_4I_W+Q_W(t)), \end{aligned} \tag{5}$$

for all $t>W$. As before, $Q(t)=Q(R(t))$ so that $Q_W(t)=Q(R_W(t))$, to first order, and the averaged external forcing is $R_W(t)=R_i+\sigma S_W(t)$. It is assumed that all averaging takes place within the time interval (t_i,t_{i+1}), where R_i is constant. In particular, it is assumed that $\mathrm{Var}[S_W(t)]\to 0$ as $W\to(t_{i+1}-t_i)$. Note that the subscript W does not denote an expectation—it is a local average. Even though $E[S(t)]$ is zero, a realization of its finite local average will not, in general, equal zero. However, $S_W(t)$ does have a reduced variance, as one would expect of an average, equal to

$$\mathrm{Var}[S_W(t)]=\gamma(W)=\frac{\theta}{W}\left(1+\frac{\theta}{2W}(e^{-2W/\theta}-1)\right), \tag{6}$$

where θ is the ''scale of fluctuation,'' taken here to equal the time constant of 8 msec. The ''variance function'' $\gamma(W)$ has

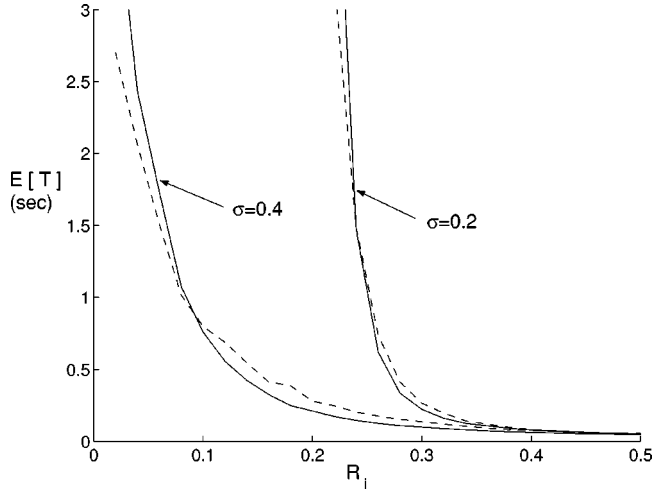

FIG. 4. The expected time to switch from State 1 to State 2, $E[T]$, found from the differential equations (1) (solid lines), is compared to that using the ''competition between averages'' model (dashed lines).

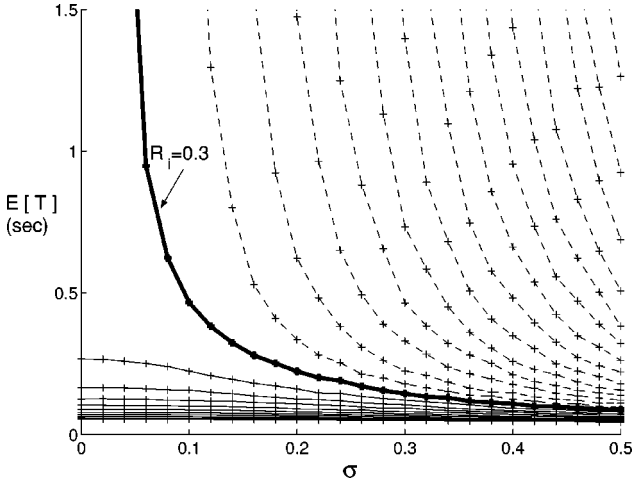

FIG. 5. The dependence of the expected time to switch from State 1 to State 2 computed from the competition between averages. The solid lines are the expected time to switch for $R_i>0.3$ and dashed lines the same for $R_i<0.3$. Note the sharp change in dependence upon σ when crossing $R_i=0.3$.

$\gamma(0)=1$ and decreases like θ/W for large W; it quantifies the variance reduction due to averaging.

The hypothesis made here is that the expected time to switching under noisy external forcing can be written in terms of the time to switching in the absence of noise, $\tau(R_i)$. That is, switching in the presence of noise occurs at a time t when *any* of the backwards averages from time t to time $t-W$ exceeds $p(W)$, where $0<W<t$ and $p(W)$ is the input threshold which leads to a switch after time W. In this scenario, imagine that each instant in time t has associated with it a continuous suite of averages stretching back to time $t=0$. If any of these averages exceeds its switching time threshold, then switching will occur at time t; each instant in time has a continuous range of local averages, $0<W<t$, from which to draw a ''winning'' threshold exceedance $R_W(t)>p(W)$. Longer times have more contributing local averages and, although longer local averages are ''weaker'' competitors due to their smaller variances, they also have lower barriers to exceed. As a result, local averages have varying probabilities of exceedance, as a function of the averaging width. Very small and very large averages tend to have small exceedance probabilities, with increased probabilities occurring at intermediate averaging widths. This is the competition between averages.

This hypothesis is verified in Fig. 4 where the expected time to switch is computed via Monte Carlo simulation using the differential equations (1) and compared to the expected time to switch obtained via Monte Carlo simulation (using a different seed) looking at backwards local averages and $p(W)$. Forcing to the differential equations is nearly white noise, as discussed previously, superimposed on R_i, and solutions are obtained using a fourth-order Runge-Kutta numerical scheme. Any errors are numerically within the magnitude to be expected from a lack of resolution of $\tau(R)$ for $R\to\infty$ and $\tau\to\infty$. The agreement between the two approaches is startling. What this means is that the differential equations are essentially integrators, accumulating sufficient energy from the input until switching is achieved.

To motivate the analysis of switching times to follow, the switching times are again depicted in Fig. 5, but now for curves of constant R_i. Here, the effect on expected switching times from State 1 to State 2 arising from both the mean level R_i and the input variance is shown. The boundary between sub- and superthreshold forcing, $R_i=0.3$, clearly delineates the dependence of the expected time on the forcing R_i and the noise level σ. Curves corresponding to subthreshold inputs, $R_i<0.3$, show a strong dependence upon R_i and σ while curves corresponding to superthreshold inputs, $R_i>0.3$, show very little dependence on σ.

A semianalytical model for the expected switching time is now developed by viewing the problem as follows: each instant in time $t>W$ is ''composed'' of a continuous sequence of local averages extending backwards in time, one of which will be the local average of width W. This component, viewed as a random function moving forward in time, has an upcrossing rate over a threshold $b=p(W)-R_i$ given by

$$\nu(W)=\frac{1}{\pi\sqrt{2\theta W}}\exp\left\{\frac{-b^2W}{2\sigma^2\theta}\right\}, \tag{7}$$

when $W\gg\theta$ [24]. An ''upcrossing'' of the threshold b would result in a switch from State 1 to State 2. If upcrossings are assumed to be (at least approximately) governed by a Poisson point process, then the time T to the first crossing of the threshold b, by the local average process $R_W(t)$, is given by

$$E[T|W]=W+\frac{1}{\nu(W)}. \tag{8}$$

Since the width of the averaging window which leads to a switch is unknown and is thus treated as random, it is necessary to compute

$$E[T]=E[E[T|W]]\approx\int_0^\infty wH(w)dw + \int_{\gg\theta}^\infty\left(\frac{1}{\nu(w)}\right)H(w)dw, \tag{9}$$

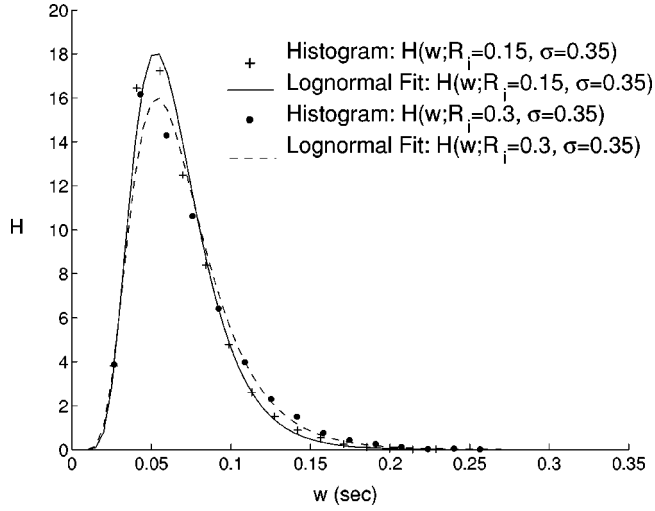

FIG. 6. The histogram of the averaging window distribution $H(w;R_i,\sigma)$, for switching from State 1 to State 2, is compared to the log-normal distribution for two subthreshold values of R_i. There is little variation in $H(w;R_i,\sigma)$ for the two values of R_i.

where $H(w)=H(w;R_i,\sigma)$ is the probability density function of W, the averaging window width which causes switching. The second integral is only asymptotically correct. Generally, values of the lower bound on the integral ranging from 5θ to 10θ have been found to yield reasonable results.

This is another statement of the ''competition between averages.'' Each average $R_W(t)$ has a certain mean first crossing time, and the likelihood that an average of width W is the one which leads to a switch (earliest crossing) is captured by H. The nature of H allows the identification of cause and effect—the amount of past input (W) which leads to a switch is now probabilistically characterized, a feature not available in energy models. The clinical relevance of this characterization appears later.

A primary analytical difficulty is that no results appear to be currently available for H. Hence, a numerical description is used to describe the properties of H for the subthreshold range $R_i<0.3$ along with values of σ such that $t_e \ll E[T] \ll 10$, of considerable practical interest. Simulation yields the following observations.

(i) H is closely approximated by a log-normal distribution. In fact, based on samples of size 500, the Anderson-Darling goodness-of-fit test results in rejection of the lognormal distribution only about 15% of the time at the 10% significance level (a 10% rejection rate would be expected). Thus, it appears that the data are very nearly lognormally distributed. This is also seen in Fig. 6 where the fitted log-normal distribution is superimposed on the normalized histogram values.

(ii) To first order H is independent of the mean input R_i and this is shown in Fig. 6. This lack of dependence of H upon R_i is surprising in light of the strong dependence of the time to switch on both R_i and the noise level σ. The clinical significance of this is pointed out in Sec. V.

(iii) The dependence of H upon σ is (approximately) self-similar; i.e., if $J(w)=H(w;R_i,\sigma^*)$, then $H(w;R_i,\sigma)=(\sigma/\sigma^*)J(\sigma w/\sigma^*)$. This means that as the input noise variance σ^2 increases, the distribution H moves closer to $w=0$, implying increased likelihoods that short averages will lead to switching. This property is shown in Fig. 7.

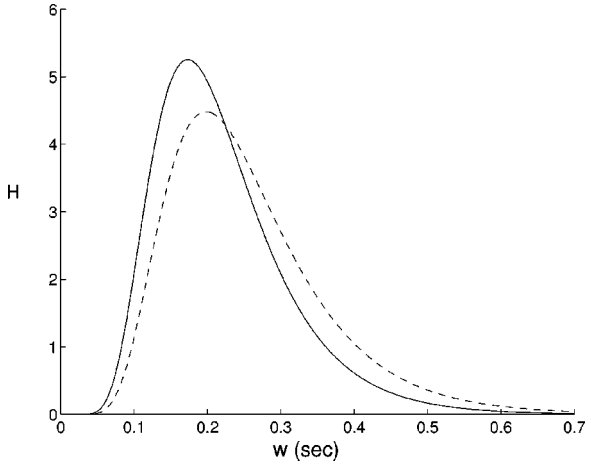

FIG. 7. The window distribution for $H(w;R_i=0.15,\ \sigma^*=0.5)$ is defined as $J(w)$ and rescaled as $\sigma/\sigma^* J(\sigma w/\sigma^*)$ (dashed line). This is compared to the window distribution $H(w;R_i=0.3,\ \sigma=0.1)$ (solid line).

These properties imply that it is only necessary to numerically estimate H for one (nonzero) input noise variance, and then H can be scaled to yield results at other variances, valid for any $R_i<0.3$ to describe switching from State 1 to 2. The agreement between this semianalytical formulation and the backwards averaging model is shown in Fig. 8 for three different values of R_i.

For superthreshold inputs $R_i>0.3$, H loses its nice properties. In particular, it becomes highly dependent on R_i and is no longer (approximately) self-similar with respect to σ. However, it tends to be approximately normally distributed around $\tau(R_i)$, so that, to first order, a reasonable approximation to the expected switching time is simply $E[T]=\tau(R_i)$. In this case, the expected time to switch is approximately independent of σ because the function $p(\tau)$ is approaching a vertical asymptote near $p=O(1)$, where changes in p do not change τ significantly.

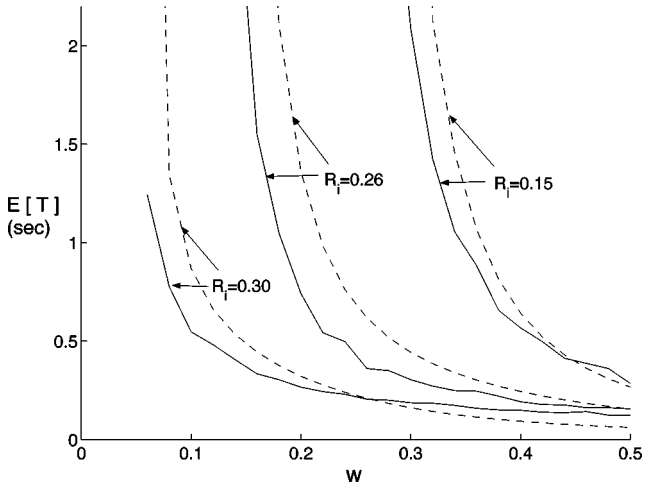

FIG. 8. The expected time to switch from State 1 to State 2 from the competition between averages (solid lines) is compared to the same predicted from the semianalytic model in Eq. (9) (dashed lines).

V. CONTROL PERFORMANCE AND CLINICAL RELEVANCE

The intrinsic cardiac nervous system contains three components [16,18]: (i) afferent neurons (for feedback from cardiac tissue), (ii) populations of densely interconnected excitatory and inhibitory neurons (each population forms a so-called ''local circuit''; neurons within a local circuit have been referred to here as ''local circuit neurons,'' and (iii) efferent neurons, which return control inputs back to the heart, made up of parasympathetic efferent neurons (to reduce cardiac output), and sympathetic efferent neurons (to increase cardiac output). This nervous system, residing on the heart, modifies regional cardiodynamics and can function independently of more centrally located neurons [17]. Indeed, arbitrary rearrangements of small portions of local circuit neurons can lead to disorganized cardiac electrical behavior which, in turn, can lead to ventricular fibrillation [25]. Hence, the intrinsic cardiac nervous system has been characterized as a *little brain of the heart* [16,19].

In the simplest closed loop controller, cardiac afferent neurons provide feedback to neurons in higher centers, such as the spinal cord and brain, where more control inputs are computed and fed back to the heart via the parasympathetic and sympathetic efferent neurons. In addition, it is believed that the intrinsic cardiac nervous system actively regulates regional cardiac function via the local circuit neurons receiving inputs for instance, from the intrinsic cardiac afferent neurons [16,19]. As discussed previously, these local circuit neurons qualitatively exhibit hysteresis (Fig. 1).

The usefulness of the description provided by ASR of local circuit neurons exhibiting hysteresis stems from the fact that it provides a means of dealing with the many noisy inputs impinging on the intrinsic cardiac nervous system. These inputs come from cardiac afferent neurons with sensory neurites in cardiac tissue and cardiac efferent preganglionic neurons in higher centers. In such an environment, hysteretic local circuit neurons serve to actively filter afferent and higher center neuronal inputs by mapping them to a finite set of states before they modify the parasympathetic and sympathethic efferent neurons regulating regional cardiac function. The importance of such filtering to maintaining control in a noisy environment is intuitively clear—the noise itself must not control the system. In fact, in addition to filtering noise, hysteretic local circuit neurons *use* noise to increase the range of inputs available for regional cardiac control, including inputs that would otherwise be considered subthreshold in the absence of noise. Thus, a broader dynamical range is available to regulate cardiac output via changes in cardiodynamics.

In a closed loop controller utilizing a hysteretic system, the main requirements placed upon the hysteretic portion, consistent with good control performance are, qualitatively, (i) an expected time to switch states that does not exceed an upper limit, ensuring a rapid enough reaction to changing control requirements, and (ii) an expected time to cycle between states that does not go below a lower limit, to suppress unwanted cycling.

Associated with these ''expected time'' requirements are similar requirements on probability. For example, even though the expected time may be acceptable, control may not be considered to have been achieved if 10% of the switching times are excessively long (with obvious consequences). Knowledge of the switching rates and distribution H allows such probabilities to be assessed, although in this work only expected times are considered. It is assumed that adequate limits on mean switching times will ensure adequate probabilistic behavior, an assumption that requires more study to fully verify.

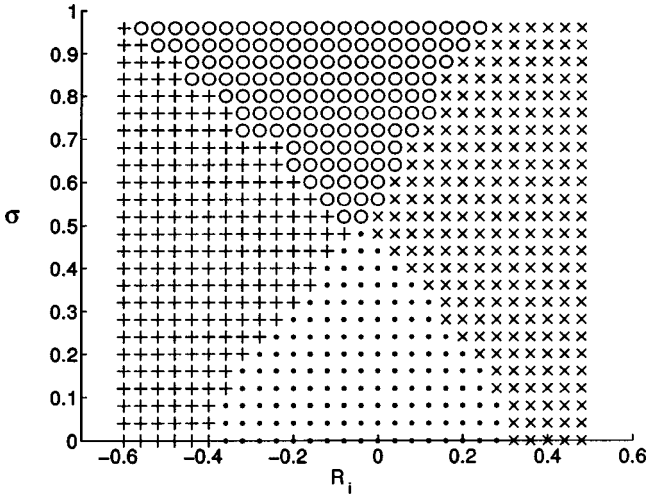

FIG. 9. Control states depicted as a function of constant input forcing R_i and noise level σ. Three states are considered: ''sleep'' (dots) for inputs that do not result in a change of state, ''active control'' ($\times$'s for τ_{12} and $+$'s for τ_{21}) where control inputs result in the desired change of state, and ''no control'' (open circles) where control inputs result in uncontrolled cycling between states.

A simple rule which partially satisfies both of these expected time requirements is that the time to switch should be much smaller than the time to cycle. Figure 9 illustrates the various control states as regions of a plot. The portion shown with dots ($\cdot$) corresponds to a ''sleep'' (passive control) state where 1-2 and 2-1 switching times are both very large, and thus effectively infinite. In other words, the system is not being driven. Directly above this region is a region marked with open circles, where the 1-2 and 2-1 switching times are both small so that (no control) cycling is taking place. The noise is completely swamping any signal that might be present, and is strong enough to be interpreted as a deterministic signal by the controller. At the left, marked with $+$'s, is the region where the 2-1 switching time is small, while the 1-2 switching time is effectively infinite. This is an active control region. Similarly, the right hand side, marked with $\times$'s, is where 1-2 switching occurs rapidly while the 2-1 switching time is effectively infinite. This region also corresponds to active control.

There are two major points of interest in Fig. 9. First of all, noise levels in the range 0.4–0.5, allow for control over the full range of possible inputs, and there is no need for noise ''tuning.'' That is, the system does not need to actively adjust the noise level for optimum performance. This observation is consistent with similar findings for many sensory neurons which are functionally in parallel [1]. Second, at somewhat higher noise levels ($\sigma > 0.5$), superthreshold control is not symmetrically jeopardized. For example, if $\sigma = 1.0$ and $R_i = 0.4$, then ''active'' control is achieved and the

system switches from State 1 to State 2. However, to return from State 2 to State 1, R_i must be decreased down to less than about -0.6, which is *twice* as far from the corresponding upper threshold. Anything short of this results in a ''no control'' state of erratic cycling. This point may be of clinical significance if switching from State 1 to State 2 is taken to represent an increased activity level and State 2 to State 1 is a reduction in activity. The physical analogy would be that increased activity is less susceptible to loss of control than the return to a reduced level of activity. This phenomenon may be clinically applicable to the occurrence of a heart attack in an individual soon after the cessation of demanding physical activity.

Another clinically relevant issue arising out of this work is that neural inputs and outputs arising from a hysteretic system can now be assessed for cause and effect. It is of considerable interest to know just what change in neural input results in a change in the output state, particularly when subthreshold inputs occur. This is a question that traditional energy methods are not designed to answer. In the model presented here for expected time to switch Eq. (9), information relating to cause and effect is contained in the probability density function H. This function specifies a likely range of averaging window widths which lead to a state change. So, for example, Fig. 6 implies that switching is a result of inputs no more than about 0.15 sec into the past, with high probability, and most likely due to inputs within about the last 0.05 sec. In essence, the competition between averages is identifying cause and effect via the probability density function H. This holds true at both subthreshold and superthreshold levels of forcing.

VI. SUMMARY AND CONCLUSIONS

Aperiodic stochastic resonance (ASR) was used here to describe state switching for a hysteretic system in the presence of aperiodic noisy forcing. The hysteretic system was assumed to have two stable states and there were also two dependent variables, i.e., that of the excitatory and inhibitory neural activities. The hysteresis was first reduced to one independent variable by expressing one forcing function in terms of the second. The noisy input problem was then described in terms of the noise free problem via a ''competition between averages.'' This occurred because of the averaging nature of the governing differential equations which essentially smooths the white noise input. A semianalytical model was developed to explain switching times in terms of the competition between averages and the probability distribution governing the averaging window responsible for a switch in states was derived. Knowledge of this distribution is clinically relevant as it may facilitate the assessment of cause and effect (this is not available with more traditional energy approaches). For example, although subthreshold switching times are dependent upon both the distance between the mean input and the switching threshold and the input noise level, the mean averaging window size leading to switching is dependent only on the noise level. In other words, cause and effect, at subthreshold inputs, may be determined solely by the noise level.

ASR was applied here to further our understanding of the effect of external noise on a densely interconnected population of inhibitory and excitatory neurons that exihibits hysteresis. The specific application was to the intrinsic cardiac nervous system. ASR predicts that, in this system, external noise can lead to an enhancement of the regulation which intrinsic cardiac neurons exert on regional cardiac function. In addition, the ASR model predicts that the relationship between adequate control performance and noise is dependent on the switching state direction when the noise is high. In fact, given an input at a fixed distance ''beyond'' a threshold, adequate control may be realized when switching states in one direction but lost in the reverse direction.

ACKNOWLEDGMENTS

Thanks are due to the National Sciences and Engineering Research Council of Canada (NSERC) for their operating grant funding G.C.K. and G.A.F., as well for financial support for K.C. Thanks are also due to the Medical Research Council of Canada for their grant to J.A.A. Finally, the authors would like to thank Dr. Andrew C. Fowler for his helpful comments on this paper.

[1] J.J. Collins, C.C. Chow, and T.T. Imhoff, Nature (London) **376**, 236 (1995).
[2] F. Moss, D. Pierson, and D. O'Gorman, Int. J. Bifurcation Chaos Appl. Sci. Eng. **4**, 1383 (1994).
[3] J.J. Collins, C.C. Chow, and T.T. Imhoff, Phys. Rev. E **52**, 3321 (1995).
[4] M.T. Mahato and S.R. Shenoy, Phys. Rev. E **50**, 2503 (1994).
[5] A. Longtin, J. Stat. Phys. **70**, 309 (1993).
[6] C. Heneghan, C.C. Chow, J.J. Collins, T.T. Imhoff, S.B. Lowen, and M.C. Teich, Phys. Rev. E **54**, 2228 (1996).
[7] A.R. Bulsara and A. Zador, Phys. Rev. E **54**, 2185 (1996).
[8] J.E. Levin and J.P. Miller, Nature (London) **380**, 165 (1996).
[9] P.C. Gailey, A. Neiman, J.J. Collins, and F. Moss, Phys. Rev. Lett. **79**, 4701 (1997).
[10] H.A. Kramers, Physica (Amsterdam) **7**, 284 (1940).
[11] C.C. Chow, T.T. Imhoff, and J.J. Collins, Chaos **8**, 616 (1998).
[12] J.J. Collins, T.T. Imhoff, and P. Grigg, J. Neurophysiol. **76**, 642 (1996).
[13] A. Krawiecki and A. Sukiennicki, Chaos **8**, 768 (1998).
[14] J.J. Collins, C.C. Chow, A.C. Capela, and T.T. Imhoff, Phys. Rev. E **54**, 5575 (1996).
[15] H.R. Wilson and J.D. Cowan, Biophys. J. **12**, 1 (1972).
[16] J.A. Armour, in *Reflex Control of the Circulation*, edited by I.H. Zucker and J.P. Gilmore (CRC Press, Boca Raton, FL, 1991).
[17] J.L. Ardell, C.K. Butler, F.A. Smith, D.A. Hopkins, and J.A. Armour, Am. J. Physiol. **260**, 713 (1991).
[18] M. Horackova and J.A. Armour, Cardiovasc. Res. **30**, 326 (1995).
[19] W.C. Randall, R.D. Wurster, D.C. Randall, and S.X. Xi-Moy, in *Nervous Control of the Heart*, edited by J.T. Shepherd and S.F. Vatner (Harwood Academic Publishers, Amsterdam, 1996).
[20] J.A. Armour, K. Collier, G. Kember, and J.L. Ardell, Am. J. Physiol. **274**, 939 (1998).
[21] A.Y.K. Wong and J.A. Armour, Neural Networks **5**, 35 (1992).

[22] Depending on the parameters and the nature of the sigmoidal response functions S_e and S_i, Eq. (1) can have hysteresis curves with more than two approximately constant steady ''States'' [15] (the capital S implies an approximately constant level is a State output analogous to State 1 or State 2 detailed in Fig. 2). The general description of a State requires only the time $\tau(R)$ to switch into that State from any State below (of smaller steady value) or above (of greater steady value).

[23] The time τ to switch states is also dependent to the order of the neuronal time constants on the initial conditions and details for when the solution of Eq. (1) is deemed to have switched states. Hence, τ is resolved to the order of the neuronal time constants.

[24] E. Vanmarcke, *Random Fields* (MIT Press, Cambridge, MA, 1984).

[25] J.A. Armour, Cardiovasc. Res. **41**, 41 (1999).